Publ. Astron. Soc. Japan 26, 387-398 (1974)

The 35 GHz Solar Interferometer at Nagoya

Kin-aki KAWABATA, Hideo OGAWA, Yoshiaki SOFUE, and Ikuro SUZUKI

Department of Physics, Nagoya University, Chikusa, Nagoya

(Received 1973 December 4; revised 1974 March 11)

Abstract

An eight antenna adding interferometer at 35 GHz (8.6 mm wavelengths) has been constructed at the Department of Physics, Nagoya University. Each antenna consists of a fixed paraboloidal reflector with a Cassegrain feed system and of a steerable plane reflector. The eight plane reflectors of equatorial mounting are aligned along an east-west line with an equal spacing. Each paraboloidal reflector is fixed pointing downwards in such a way that the axis of the paraboloidal reflector coincides with the polar axis of the equatorial of each plane reflector. This system of antennas eliminates the need for the waveguide rotary joints and is usable even in rainy days.

The interferometer has a total span of 16.38 m (1913λ). The angular resolution and the scanning time interval are 1.4′ and about 50 s respectively at the meridian transit of the sun. Observations of the sun are regularly performed about 10 hr each day in summer and about 7 hr in winter.

We discuss the performance of the interferometer in some detail and illustrate examples of observations.

Key words: Solar flare; Solar millimeter-wave burst; Solar radio interferometer; Sunspot.

1. *Introduction*

An eight antenna east-west interferometer at 35 GHz (8.6 mm wavelengths) with a total span of 16.38 m has been constructed at the Departement of Physics, Nagoya University. The instrument has been constructed primarily for the purpose of studying of solar radio bursts at millimeter wavelengths. The observing site is located on the campus of the University (136°58′.3 E, 35°8′.8 N).

Accurate measurement of locations and sizes of radio bursts would be of importance in the study of solar radio bursts and to clarify physical processes involved in the solar flare complexity. In order to monitor radio bursts and to measure their locations and sizes, the instrument has to satisfy the following requirements: (i) high angular resolution, (ii) high time resolution, (iii) many operational hours, and (iv) usability on rainy days. The half-power beam-width of our interferometer is 1.4′ and the time intervals of scannings of a point source on the solar disk are about 50 s near the meridian transit. We usually make solar observations for about 10 hr each day from April through September and for about 7 hr in winter, although the half-power beam width and the scanning time interval increase at large angles from the meridian plane. Our antenna is usable even on rainy days and observations of the sun have been performed for about 8200 hr during a thirty five month period, including 240 rainy days, since we

started test observations by using two of the eight antennas.

The construction of the instrument was started in 1969 and test observations by using two antennas were made in August 1970. Observations of the sun by using four antenna interferometer were made from September 1970 through March 1971. Some results of observations by the four antenna interferometer have been reported elsewhere (KAWABATA and SOFUE 1972; KAWABATA, SOFUE, OGAWA, and OMODAKA 1973). Continuous observations of the sun by the eight antenna interferometer have been performed since April 1971. In the present paper, we describe the performance of the instrument in some detail and show some examples of observations.

2. *Antennas*

Each antenna consists of a fixed paraboloidal reflector with a Cassegrain feed system and of a plane reflector of equatorial mounting. The diameter d and the focal length of the paraboloidal reflectors are 40 cm and 10 cm respectively, and the second reflectors have a diameter of 5 cm. Each paraboloidal reflector is fixed pointing downwards along the polar axis of the respective plane reflector, which

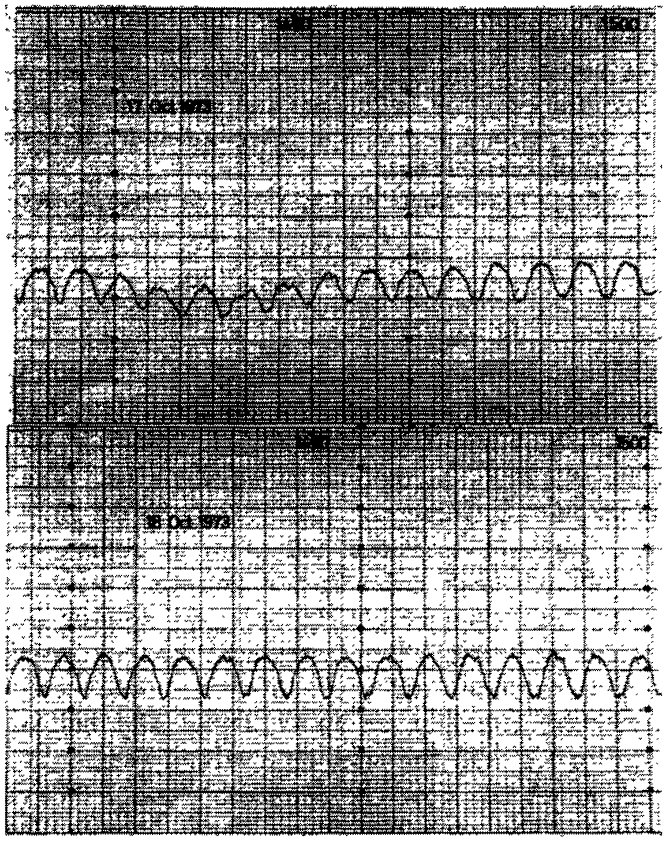

Fig. 1. Records of the interferometric observations of the quiet sun on a rainy day (upper) and a fine day (lower). The precipitation at the time of observation on 17 October 1973 was at a rate of about 5 mm hr^{-1}. The observation of the precipitation was made at the Nagoya Local Meteorological Observatory, which is located about 2 km apart from the observing site.

is placed in front of each paraboloidal reflector. The distance of the plane reflector from the opening of the paraboloidal reflector is about 46 cm and is very short compared with the Fresnel distance $d^2/\lambda=18.6$ m of the latter.

This particular system of antennas eliminates the need for the waveguide rotary joints but still allows the pointing of the antennas on the sun all the time. The present system of antennas has another advantage that observations of the sun can be performed even in rainy days. Because the Cassegrain antennas are always kept dry and the plane reflectors are uniformly drenched on rainy days, the effect of rain on the efficiency of the antennas is relatively small. Such an advantage is preferable especially at millimeter wavelengths, because any drops of water attached to the feed system of usual antennas prohibit observations. Figure 1 illustrates an example of a comparison of our data obtained on a rainy day and on a fine day. The quasi-periodical variations in the records show the interference patterns due to the quiet sun. A depression before about 14:54 JST (Japanese Standard Time) on 17 October 1973 is due to atmospheric attenuation. Since we started test observations in August 1970, the instrument has been operated about 8450 hr, including 240 rainy days, until June 1973. During the 8450 hr operations, observations of the sun were impossible for about 250 hr due to strong atmospheric attenuations or else due to rapid changes of attenuations. Except for these 250 hr, observations of the sun have been actually performed. Since radio bursts appear as periodic spikes in our records, we can easily discriminate slow changes of weak attenuations from the flux of solar radio bursts.

3. *Arrangement of Antennas*

The eight antennas are placed along an east-west line with an equal spacing of $D=234$ cm (273λ). Figure 2 illustrates spatial frequencies involved in our observations for the various values of the hour angle and declination. Abscissae and ordinates are the components of the spacial frequencies in the east-west and in the north-south directions of the equatorial coordinates respectively. In these figures, only the first quadrants are shown. The beam separation and the half-power beam-width are 12.6′ and 1.4′ respectively at the meridian plane. Figure 3 illustrates the time intervals between the grating responses of a point source on the solar disk due to drift scannings as a function of hour angles.

The antenna spacings of interferometers for solar observations are usually made a little shorter than the spacing corresponding to the diameter of the sun seen at that wavelength, i.e., less than 90λ below 10 cm wavelength. We selected as large a spacing as 273λ because of the following reasons. At millimeter wavelengths, the size of antennas becomes neccessarily large relative to the usual spacing of antennas because of the relatively high system noise temperature of the receiving system. Therefore, observations at large angles from the meridian plane will be prohibited by the obscuration of each antenna by the next one, if we select the usual separation of antennas. The large spacing of 273λ makes it possible to observe the sun for about 10 hr each day except in winter. The receiving system of our interferometer has a bandwidth of 8 MHz. The decrease of correlation due to delays in the receiving band is less than 30 percent and can be corrected for by digital data processing. The interferometer with the large spacing has another advantage in that the time resolutions are relatively high without using the beam scanning by phase shifters. The time resolution of about 50 s is not

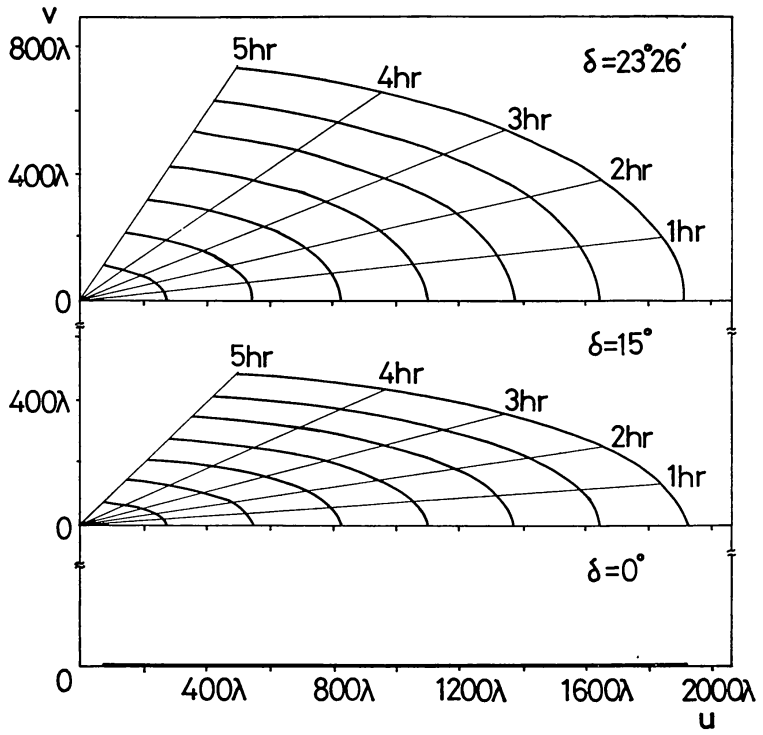

Fig. 2. Spatial frequencies involved in the 35 GHz interferometer observations. u: east-west component in the equatorial coordinates. v: north-south component. The corresponding hour angles are indicated in the figure.

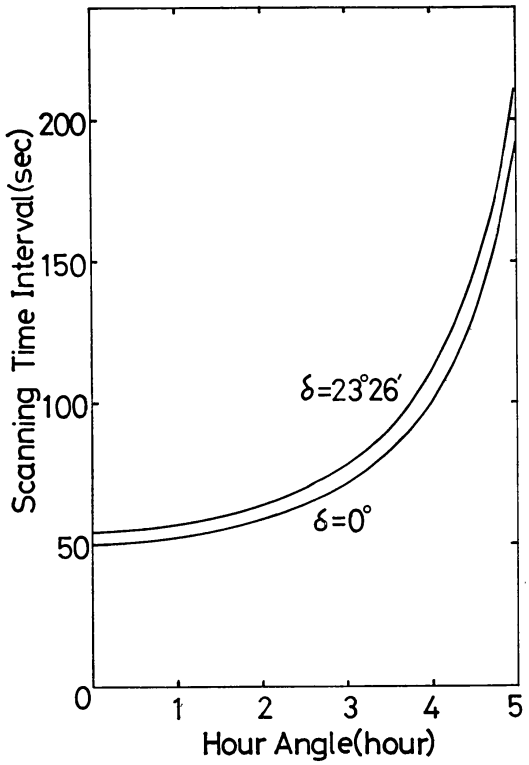

Fig. 3. The scanning time intervals.

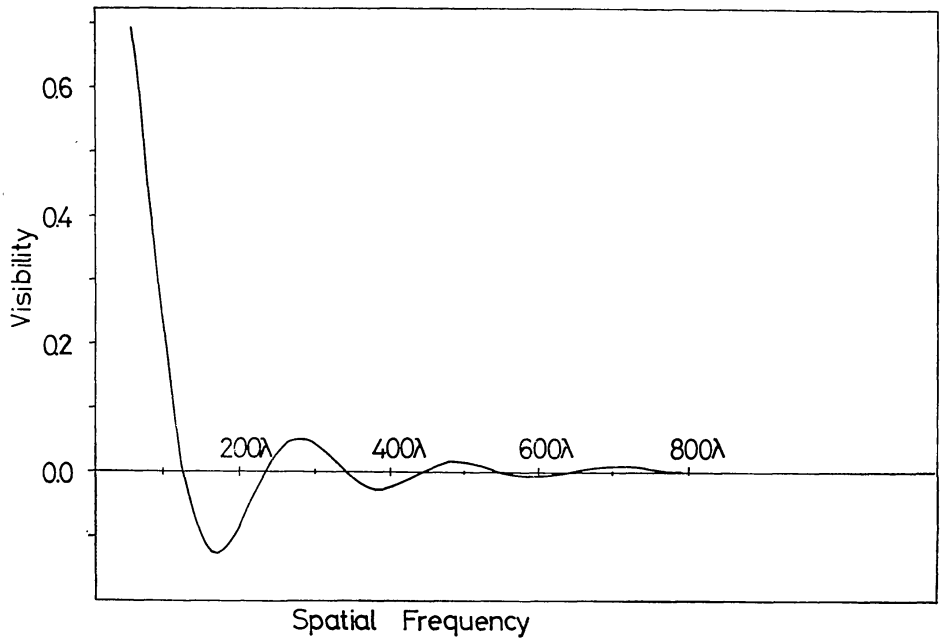

Fig. 4. Visibility function of the quiet sun at 35 GHz. The distance of the sun is taken to be 1 AU.

sufficiently high for some radio bursts, but is tolerable.

The visibility function of the quiet sun at 8.6 mm shows decaying oscillatory variations as a function of the spatial frequency, as is illustrated in figure 4 (KAWABATA and SOFUE 1972). The antenna spacing of 273λ is selected because it corresponds to the third extremum of the visibility function. In such a case, amplitude of the quiet sun interference pattern becomes relatively large at the meridian passage, especially when we observe the sun by using two adjacent antennas. The large amplitude makes it very easy to measure the phase errors of our instrument by observation of the sun. The measurement of the phase errors through 10 min observations of the sun by using two adjacent antennas gives an accuracy better than 10° in phase angles in peak-to-peak value. We are using this method for the checking of phase errors of our instrument.

TSUCHIYA (1969) has obtained the value of 3 s.f.u. (10^{-22} Wm^{-2} Hz^{-1}) as a typical flux density of the S-component at 8.6 mm. This value is only about 0.15 percent of the flux density of the quiet sun. If ten sources of S-component with a flux density of 3 s.f.u. are distributed randomly in phase angles, the presence of the sources of the S-component may produce an error of about 10° in the measurement of the phase errors. Since this value is sufficiently small and the day-to-day variation of the measured value of the phase errors is actually less than 10°, the accuracy of the determination of the phase errors through the observations of the sun is sufficiently high.

Figures 5 and 6 illustrate examples of phase departures of our instrument measured by observations of the sun on a quiet day. We give a beam number to each fan beam in the order of the hour angle. The beam number "0" corresponds to the fan beam in the meridian plane. The positive and negative signs of the beam numbers indicate that the corresponding fan beam is located on the west and east sides of the meridian plane respectively. As is seen in figure 5, our

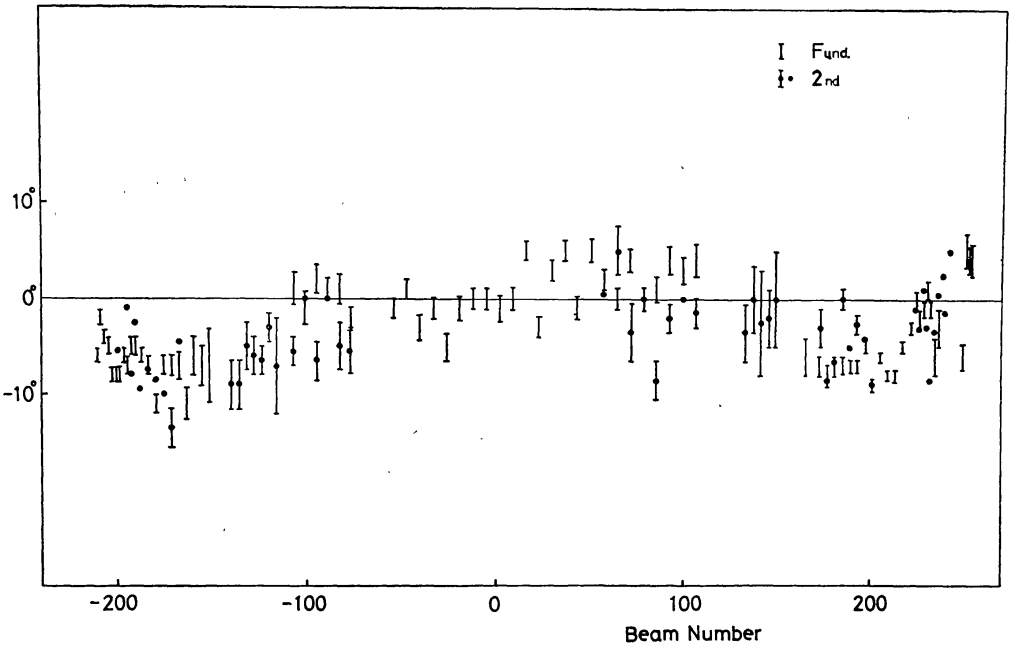

Fig. 5. An example of phase departures of the fundamental ($\mathbb{I}$) and second ($\overset{\bullet}{\mathbb{I}}$, •) spacings measured by observations of the quiet sun.

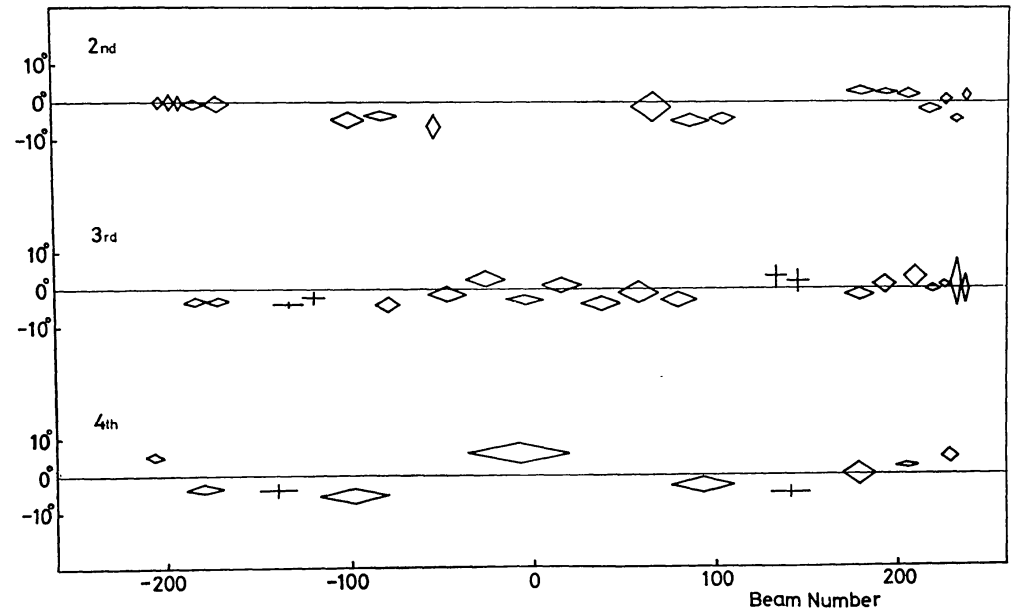

Fig. 6. An example of phase angles of the 2nd, 3rd, and 4th spacings relative to the phase of the fundamental (◇) and second (+) spacings, respectively.

interferometer may have systematic phase errors as small as about 5° even at very large angles from the meridian plane. The systematic phase error persists for more than two weeks and can be corrected for by data processing. The random fluctuations of the phase departure are less than ±5°. We usually determine the location of a radio emission region by comparison with the phase of the quiet component of the sun. In such a procedure, the phase error may produce an error of about 15″ and 30″ in the location of the radio emission region by observa-

tions close to the meridian plane and by observations far from the meridian plane respectively.

Since our interferometer has a beam separation of 12.6′ at the meridian plane, two or three fan beams may be on the solar disk simultaneously. Therefore a single scanning of a point source on the solar disk may cause an ambiguity in its location. Such an ambiguity in the location disappears for radio bursts with long durations, for example lasting more than 30 min in most cases. The beam separation and the position angle of the fan beam change as time elapses and then the location of the burst can be determined uniquely. For a burst with short duration, we can select one out of two or three locations by comparison with optical observations usually without any difficulty.

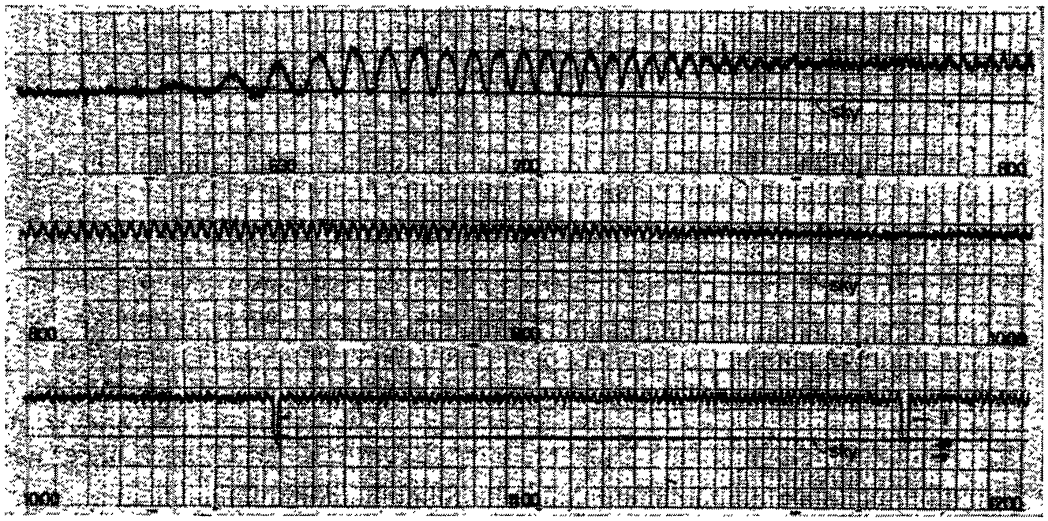

Fig. 7. Interference pattern of the quiet sun observed by the interferometer. The time in Japanese Standard Time is indicated in the figure.

The interference pattern of the quiet sun observed by our interferometer is illustrated in figure 7. The observation was made on 31 August 1972. Just after sunrise a single fan beam scans the solar disk and we can obtain an unambiguous scan curve of the quiet sun. The interference pattern almost disappears at around 07:40 and at around 10:00 JST. From 07:40 to 10:00 JST, the maximum on the record corresponds to the time when two fan beams are at symmetric position in relation to the disk center. From 10:00 to 14:00 JST, the maximum on the record corresponds to the time when a fan beam is at the disk center.

4. *Receiving System*

The block diagram of the interferometer is shown in figure 8. After the signals from two adjacent antennas are added by connecting these antennas with rectangular waveguides of the standard size, they are transmitted through rectangular waveguides about twice as large as the standard size in linear dimensions in order to reduce transmission loss. We use two Dicke type r.f. receiving systems and each of them receives signals from four of the eight antennas. The r.f. receiving systems consist of ferrite switches driven by common reference signals for Dicke modulations, band elimination filters for the rejection of image band signals in

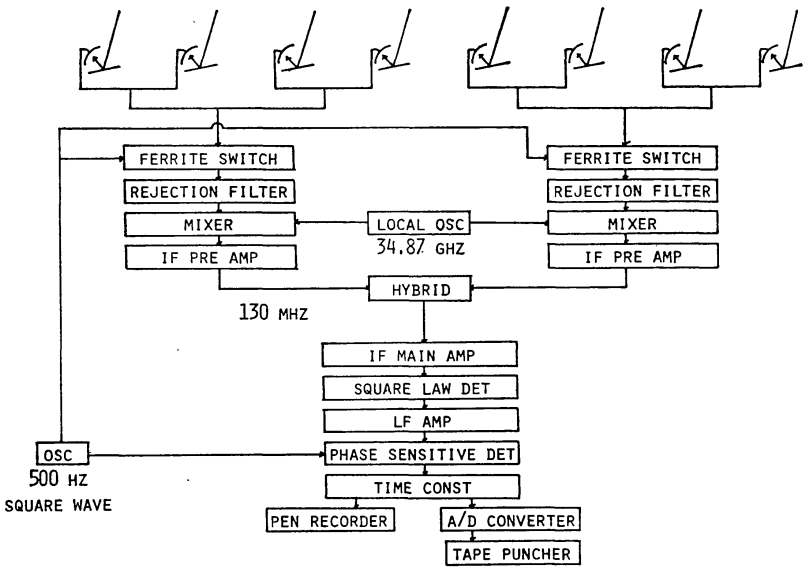

Fig. 8. Block diagram of the 35 GHz solar interferometer.

order to avoid interference from the image band, and balanced mixers operated by a common local oscillator. Finally, signals from all eight antennas are added at the intermediate frequency. The i.f. amplifiers have a center frequency of 130 MHz and a band width of 8 MHz. Observed data are usually recorded by a pen-recoder, but are sometimes also recorded on magnetic tape or paper tape for the convenience of the digital data processing. The minimum detectable flux density of a point source from a single scanning datum is about 10 s.f.u. under usual conditions of operation and is about 5 s.f.u. for good conditions.

5. *Examples of Observational Data*

We illustrate some examples of data provided by the interferometer.

(i) *20 April 1971 Event*

On 20 April 1971, the interferometer recorded a solar radio burst at 8.6 mm beginning at about 05:10 UT. Figure 9 illustrates a part of the original record of the event. The observation was performed with an integration time of 3 s. The approximately sinusoidal variation of the record is due to the quiet sun component and the humps appearing periodically nearly at the top of the quiet sun pattern are due to the radio burst. The beam separation and the half-power beam width are 15.5′, and 1.7′ respectively, at the time of the observation. The ratio of

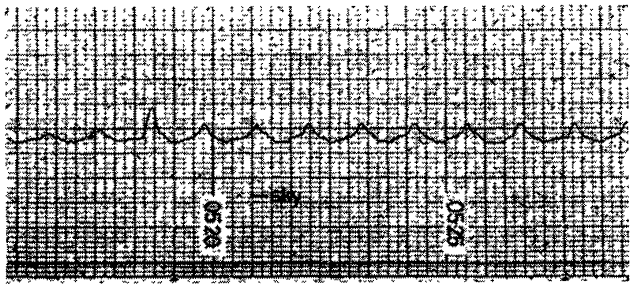

Fig. 9. Record of the 20 April 1971 event.

the flux density of the burst to that of the quiet sun is given by the ratio of the area of the excess part due to the burst to the area between the quiet sun pattern and sky level integrated over a scanning period. The flux density of the burst is obtained from this ratio by assuming that the flux density of the quiet sun is 2000 s.f.u. at 8.6 mm.

Figure 10 gives a time variation of the flux density of the present burst. Each point corresponds to each scanning. Figure 11 illustrates a comparison of the radio observation with an optical observation. The time of the radio observa-

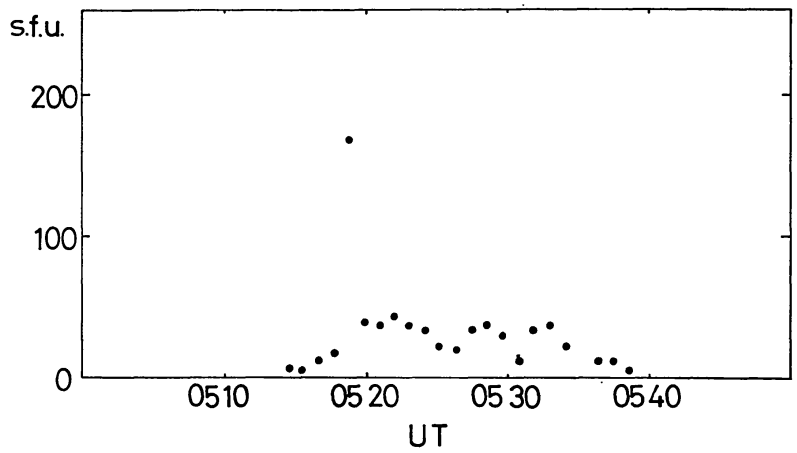

Fig. 10. Time variation of the flux density of the 20 April 1971 event.

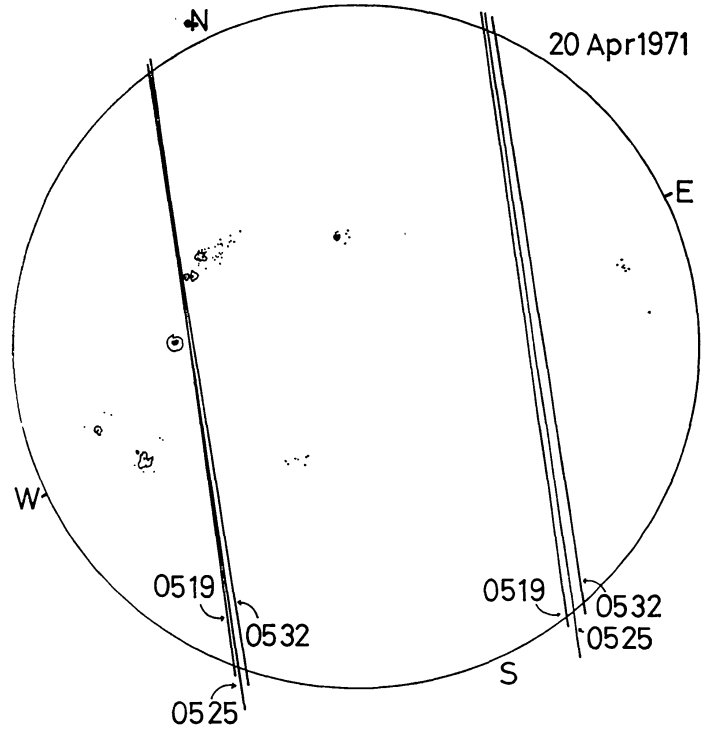

Fig. 11. Location of the radio emission region of the 20 April 1971 event. The center of radio emission region was located on straight lines at the time indicated in the figure. The straight lines in the east hemisphere are ghost images.

tion is indicated in the figure. The sketch of the sunspots was drawn from a sketch (courtesy of the Tokyo Astronomical Observatory) observed at around 00:40 UT by taking into account the rotation of the sun between the time of the radio burst and the time of the optical observation. The interferometric observation indicated that the center of the radio emissions at 8.6 mm of this burst is located somewhere on the straight lines in figure 11. In the present case, we obtain two such lines on the solar disk from a single scanning datum, as is seen in the figure. One of them (east line) is due to a ghost image, and it moves on the solar disk as time elapses because the beam separation and the position angle of the fan beam changes. On the other hand, the lines for true location (west line) coincide all the time within observational error in the northern hemisphere. In this way, we can discriminate between the ghost image and the true location. The true lines run through just the preceding side of small preceding sunspots of an active region, which have magnetic fields of class 4 ($1600 < H < 2000$ G) (*Solar Geophysical Data*, 1971 June, No. 322 Part I, p. 78). Reports on Hα flare indicated that an importance 2B flare occurred in this active region (*Solar Geophysical Data*, 1971 October, No. 326 Part II, p. 16).

Figure 12 illustrates schematically the relation between the radio emission region and sunspot magnetic field configuration. The observation indicated that the radio emission region was located on the central line. Lines on both sides indicate the error of observations. If we suppose that the radio emission region is located just above the umbras, the height of the radio emission region might

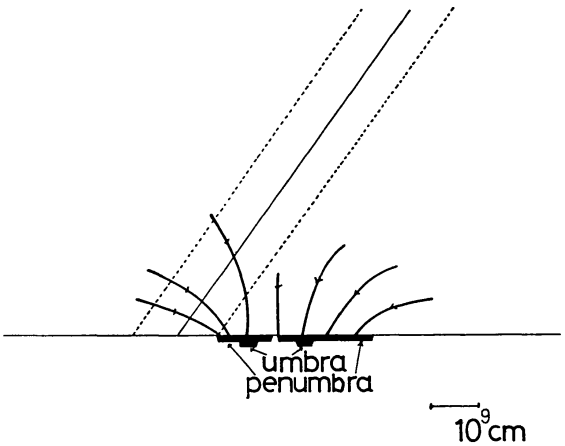

Fig. 12. A schematical representation of the configuration of sunspot magnetic fields and a radio emission region for the 20 April 1971 event. The thick lines represent magnetic lines of force. The thin line represents the line of sight through the radio emission region. The dotted lines represent the range of errors of the observations.

be higher than 10,000 km. Another interpretation is that the radio emissions are highly directive in the plane perpendicular to the magnetic field.

(ii) *2 August 1972 Event*

Figure 13 illustrates an example of a comparison of data recorded on a magnetic tape and the quiet sun interference pattern. The comparison is made by using a computer OKITAC 4300. The radio burst at 8.6 mm started before 21:27 UT and probably after 21:20 UT, and attained its maximum flux density of 955 s.f.u. at

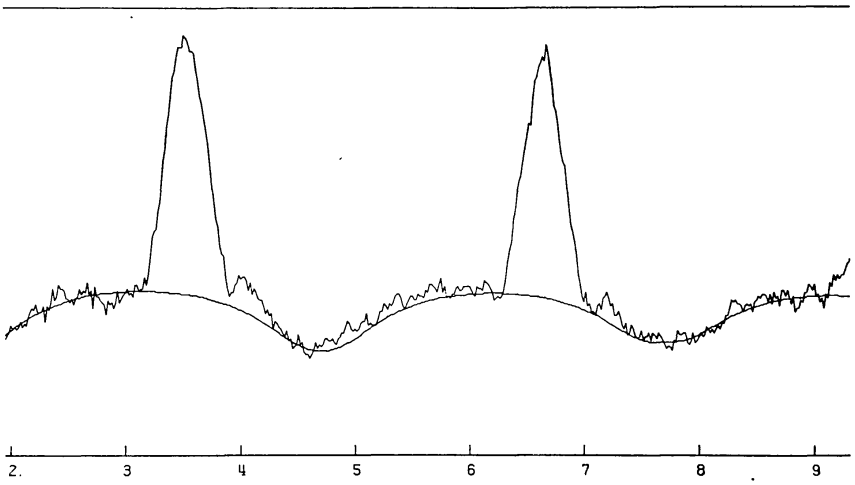

Fig. 13. Record of the 2 August 1972 event and the quiet sun interference pattern.

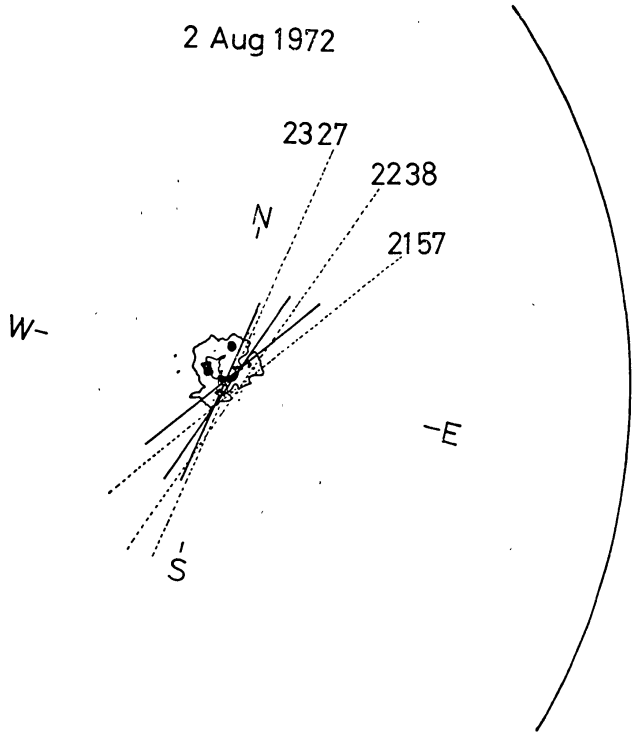

Fig. 14. Location of the radio emission region of the 2 August 1972 event. The dark area in the figure indicates umbral region of the sunspots and the curved lines surrounding umbral region indicate the outer boundaries of the penumbral region. The arc at the right represents the limb of the sun. The sketch of the sunspots was drawn at around 00:25 UT on 3 August 1972. The radio emission region was located on a dotted line relative to the limb at the time indicated in the figure. If we take into account the rotation of the sun between the time of the optical and of the radio observations, the radio emission region was located on the solid lines relative to the sketch of the sunspots. All of the solid lines cross at the sourthern part of the sunspot group.

around 21:45 UT. Some of the data provided by the interferometer on this radio burst were reported by OGAWA and KAWABATA (1973).

The quiet sun interference pattern (the smooth line in figure 13) is calculated by using an expression on the brightness distribution $B(r)$ of the quiet sun

$$B(r)=\sum B_i J_0(\mu_i r/R) \quad \text{for} \quad r\leq R\ ,$$

where B_i are parameters determined observationally (KAWABATA and SOFUE 1972). Here r denotes the distance from the disk center and μ_i denote i-th zeros of the zero-order Bessel function. R is taken to be $1.2R_\odot$. The visibility function calculated by using parameters B_i assumed in the data reduction is illustrated in figure 4.

Figure 14 illustrates a comparison of the location of the radio emisson region with a sketch of the sunspots (courtesy of the Tokyo Astronomical Observatory). The sketch of the sunspots is drawn at around 00:25 UT on 3 August. The radio data indicated that the center of the radio emission was located somewhere on the dotted line. In this comparison with the sketch of the sunspots, the rotation of the sun between the time of the radio and optical observations is not corrected for. When we take into account the rotation of the sun, the location of the center of the radio emission moves to the solid line relative to the sunspots. All of the solid lines cross at the southern part of the sunspot group as is seen in the figure, suggesting that the center of the radio emission was located at the crossing point. ZIRIN and TANAKA (1973) noted a brightening in the Hα and 3835 lines close to the cross of our observations. The radio observations may suggest that the brightening in the Hα and λ 3835 lines in this region is connected with the radio burst.

The authors would like to thank Professor I. Kondoh for his advice on digital data processing. They also wish to express their thanks to Mr. K. Akita for his assistance in the construction of the interferometer, in the observations, and in the data processings.

References

KAWABATA, K., and SOFUE, Y. 1972, *Publ. Astron. Soc. Japan*, **24**, 469.
KAWABATA, K., SOFUE., Y., OGAWA, H., and OMODAKA, T. 1973, *Solar Phys.* **31**, 469.
OGAWA, H., and KAWABATA, K. 1973, *Rep. Ionosph. Space Res. Japan*, **27**, 153.
TSUCHIYA, A. 1969, *Solar Phys.*, **7**, 268.
ZIRIN, H., and TANAKA, K. 1973, *Solar Phys.*, **32**, 173.